Fermilab

RECINTO UNIVERSITARIO DE MAYAGÜEZ
CAAM
UNIVERSIDAD DE PUERTO RICO

Determining Stability Margins in Adiabatic Superconducting Magnets with 3-D Finite Element Analysis

Author:
Arnaldo Rodríguez González
Department of Mechanical Engineering
University of Puerto Rico at Mayagüez

Supervisor:
Tengming Shen, Ph.D.
Superconducting Materials Department
Fermi National Accelerator Laboratory

SIST Program 2012

Table of Contents

Abstract 2

Introduction 2

MATLAB prediction program & the MIITS method 4

FEA simulation 8

Pre-solving method 8

Solving method 10

Tested cases 12

Single-strand case 12

Multi-strand case 13

Results 15

FEA vs. MIITS 15

Minimum Quench Energy 17

Conclusions 18

Future use 19

Acknowledgements 19

References 20

Abstract

Superconducting magnets play a key role in the development of experiments at Fermilab; understanding the operating stability of these can allow us to utilize more potent magnets for future experiments (like the proposed Muon Collider), optimize the design of magnets in more immediate experiments (like Mu2e), and research the future use of more exotic materials (like high-temperature superconductors). This summer, I developed a 3-D parametric FEA program in ANSYS Mechanical APDL that simulates quench in superconducting magnets, and I also developed a parametric MATLAB program that predicts thermal behavior in magnet quench using the MIITS method. These programs can provide useful quenching parameters (like minimum quench energy and normal zone propagation velocity) for different cases of quench, leading to the previously mentioned objective of magnet design optimization. To test the programs, preliminary cases were run and the data produced was compared and analyzed. The results of these analyses, as well as the program operating methods, are discussed in this project.

Introduction

Superconductivity, discovered in 1911 by Heike Kamerlingh Onnes, is a quantum mechanical phenomenon where a material shows zero electrical resistivity and expulsion of internal magnetic fields below a characteristic critical temperature T_c. This effect is extremely useful for high-field magnet applications: since no Joule heating in the electromagnet is generated regardless of operating current, very high-intensity fields can be generated due to high operating currents in the magnet itself. This application was pioneered here at Fermilab with the Tevatron, and the technology has branched out into various other fields, like MRI (Magnetic Resonace Imaging) machines and mass spectrometry. However, it does come with certain operating risks, the biggest possibly being quench.

Quenching in superconductors occurs when a section of the superconductor snaps out of the superconductive state and become normally resistive. Because of this, Joule heating is generated in this section, which then expands the normal zone and causes a chain reaction in which the entire conductor becomes resistive. This, if left, unchecked, can easily damage or destroy the magnets and any surrounding parts. A quench event can be initiated if any of the three following things occurs:

1) The temperature of any section of the magnet exceeds the critical temperature T_c .
2) The current of any section of the magnet exceeds the critical current $I_{c\,.}$
3) The magnetic field through any section of the magnet exceeds the critical field H_c .

Interestingly enough, these values are coupled: operating the superconducting magnet at a higher temperature, for example, yields a smaller I_c . This coupling causes behavior that not only takes into consideration quench due to critical temperature, but also due to other parameters (like critical current) which change due to changes in operating conditions. In most composite magnets, this leads to current sharing.

Current sharing is a phenomenon that occurs when a composite superconductor (generally described as superconducting filaments encased in a normally resistive matrix) surpasses the critical current for its operating temperature. Due to this, a certain portion of the current leaps out of the superconductor and flows through the matrix, creating Joule heating. Since the values of critical current, critical field and critical temperature are coupled, and current sharing is mediated by the critical current, it's possible to determine a current sharing temperature T_{cs} that specifies when current sharing behavior starts for a constant operating current, operating magnetic field, and initial temperature. The equation that determines this is below.

$$T_{cs} = T_{c0}\left(1 - \frac{B}{B_{c0}}\right)^{0.59} - \left(\left(T_{c0}\left(1 - \frac{B}{B_{c0}}\right)^{0.59}\right) - T\right)\frac{I_o}{I_{c0}}$$

(Eq. 1)

This current sharing temperature depends on multiple values: it depends on the critical temperature at zero field T_{c0}, the critical field at zero degree B_{c0}, the critical current at zero field I_{c0}, the operating current I_o, the operating field B, and the initial operating temperature T. This T_{cs} variable is the variable directly used in the simulation to determine when current sharing behavior starts. Of note is the fact that the phenomenon is dependent on the temperature of the superconducting filament/s: but the heating itself is dependent on the temperature of the matrix, since the resistivity is temperature-dependent.

MATLAB prediction program & the MIITS method

To estimate the thermal behavior of the magnet for various cases in a quick fashion, a prediction program was developed in MATLAB that uses conditions similar to the simulated case. The prediction program uses numerical integration among other techniques to quickly approximate the behavior of the maximum hot spot temperature in the conductor as a function of time, centering the solution process around the MIITS method. It does the calculation based on the following equation:

$$A_{cd}C_{cd}(T)\frac{dT}{dt} = \frac{\rho_m(T)}{A_m} I^2{}_{op}(\mathrm{t})$$

(Eq. 2)

This equation describes adiabatic heating in a constant-current mode per unit length for a homogeneous conductor with a volumetric heat capacity that is a weighted average of the heat capacities that make it up. For the following case, the composite heat capacity is determined by the following equation, where γ is the ratio of matrix material to superconductor:

$$C_{cd} = C_m\left(\frac{\gamma}{\gamma+1}\right) + C_{sc}\left(\frac{1}{\gamma+1}\right)$$

(Eq. 3)

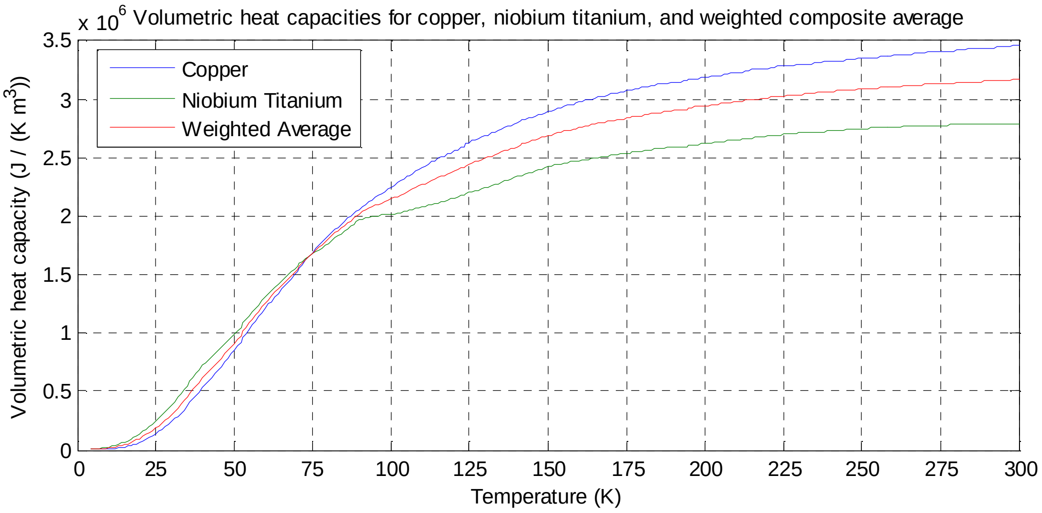

Figure 1: Heat capacities for Cu, NbTi and weighted average with γ = 1.3

Inserting the term $J_m = I_{op}/A_m$ (Eq. 4) and understanding that $A_m/A_{cd} = \frac{\gamma}{\gamma+1}$ (Eq. 5), the equation is transformed into:

$$C_{cd}(T)\frac{dT}{dt} = \left(\frac{\gamma}{\gamma+1}\right)\rho_m(T)\,J^2{}_m$$

(Eq. 4)

Rearranging the equation so that temperature-dependent terms are together and performing appropriate integration, the result is:

$$\int_{T}^{T_f} \frac{C_{cd}(T)}{\rho_m(T)} dT = \left(\frac{\gamma}{\gamma+1}\right) J^2{}_m t$$

(Eq. 5)

The right side of the equation has been considerably simplified by assuming that the initial time is zero and the current density in the matrix is constant over time; therefore, the MIITS method prediction does not take into account current sharing behavior at all.

The left-hand side of this equation is very important: this parameter, known as the Z function where $Z(T_f, T) = \int_{T}^{T_f} \frac{C_{cd}(T)}{\rho_m(T)} dT$ *(Eq. 6)*, describes a characteristic curve which shapes the thermal behavior of the conductor for any applied current. Thermal curves differing from one another for various cases with same conductor materials are only due to the scaling factor $\left(\frac{\gamma}{\gamma+1}\right) J^2{}_m$, which depends on the operating current and on the ratio of matrix to superconductor of the strand.

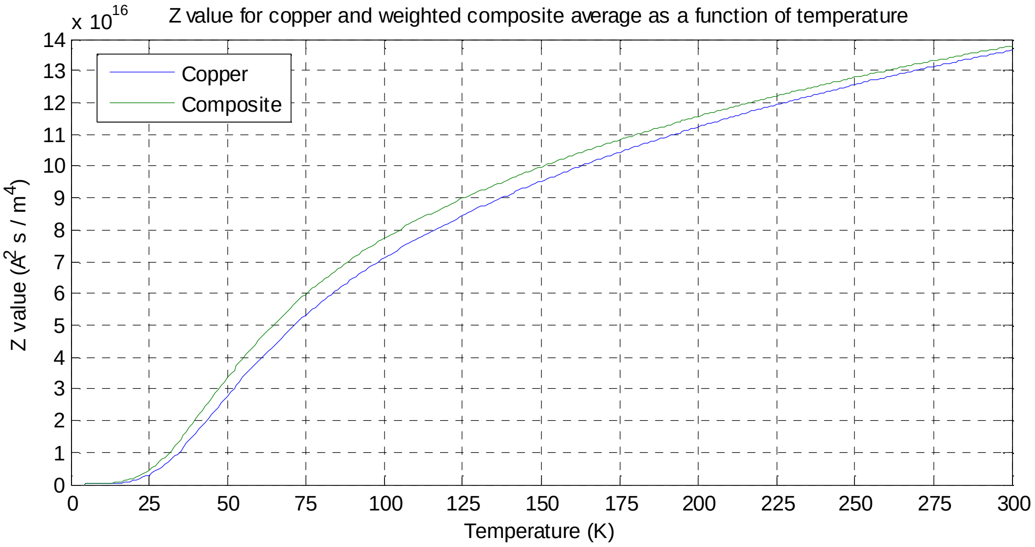

Figure 2: Z plots for copper and weighted composite average with γ = 1.3

This prediction program, like the simulation, is parametric: the program asks for key values as initial input and then performs the calculation based on these. This allows for multiple predictions to be made based on a changing single parameter, like operating current, and for their behavior to be compared. An example of predictions based on changing parameters is shown below, in this case for a changing reduced current (operating current to critical current ratio).

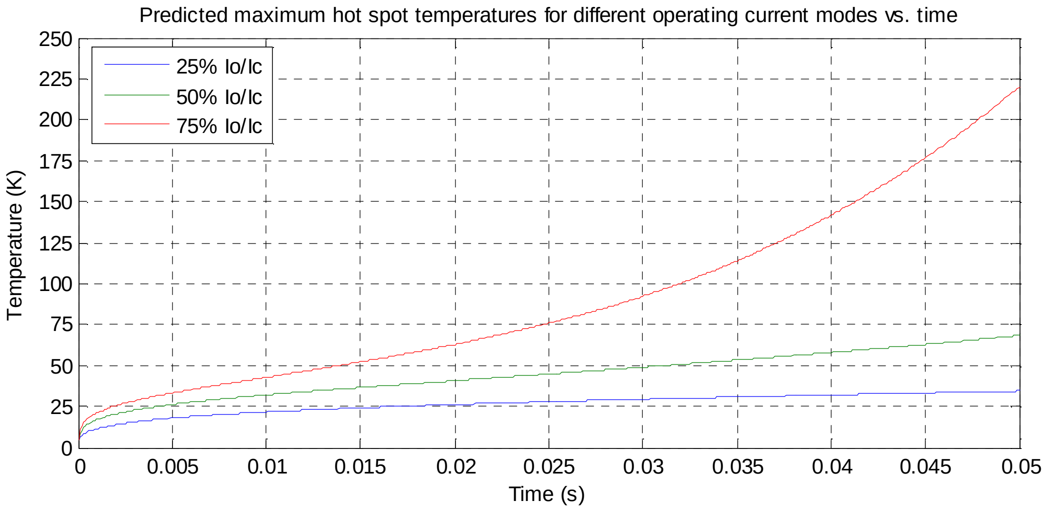

Figure 3: MIITS predictions for varying operating currents

However, the prediction program has its limitations: as previously mentioned, it does not take into account either current sharing behavior or thermal diffusion. Whether or not the current sharing phenomenon changes the behavior of the temperature drastically in comparison to the prediction is discussed in the results section. Also, the prediction program assumes the distribution of material in the conductor is uniform in its cross-section. This can cause deviations in the comparison between simulated temperature and predicted temperature due to an increasing temperature difference between the matrix and the superconductor as a result of differing heat capacities.

FEA simulation

To be able to account for these behaviors and conditions, a parametric FEA simulation was developed in ANSYS Mechanical APDL 14 that simulates quench in superconducting magnets of variable geometries and under variable conditions. The equation that governs the quench phenomenon in the FEA simulation is a power density equation, defined as:

$$C(T)\frac{dT}{dt} = \nabla \cdot (k\nabla T) + J^2\rho(T) + h_{initial}$$

(Eq. 7)

This equation incorporates both thermal conductivity and the initial heat pulse into the solution, unlike the MIITS program. It also allows for variations in the cross-section of the strand, since the equation describes power per unit volume instead of per unit length as in the MIITS case. In fact, one can derive Equation 4 (sans the ratio term, which wouldn't be needed in this case) from Equation 7 by removing the thermal conduction and initial heat pulse terms. However, Equation 7 by itself cannot incorporate current sharing behavior, so that behavior had to be taken into account directly by "hard-wiring" it into the FEA program. This meant that a (relatively) simple coupled-field analysis with ANSYS would not do: the electrical phenomena in the superconductor had to be manually included into the program through macros in the solution step, while ANSYS took care of the more complicated thermal phenomena. The methods used to accomplish this, as well as other important program methods, are discussed below.

Pre-solving method

The first thing that occurs in the simulation program is the assignment of values to important parameters in the simulation: these include the geometry parameters, the quench section length (which determines the disturbance spectrum of the quench), the initial heat energy input, the critical temperature and the operating current among others. Secondary values (like current sharing temperature) are calculated automatically based on these primary input variables.

The pre-solving method is as parametric as possible: soft alterations to the geometry and to other numerical parameters in the simulation do not require any additional changes to the code. However, due to the use of spatial “differentials” in the solving process (which are explained in more detail in the solving method section), it is required that finite element nodes be located at regular intervals on the z-axis. This is achieved via performing line divisions on the longitudinal line geometries prior to the meshing. (An important condition worthy of note that this creates is that the geometry is then required to be located in Cartesian coordinates and to extend longitudinally over the z-axis. If a geometrically faithful representation of a solenoid were to be built, for example, it would require significant alteration to the program.)

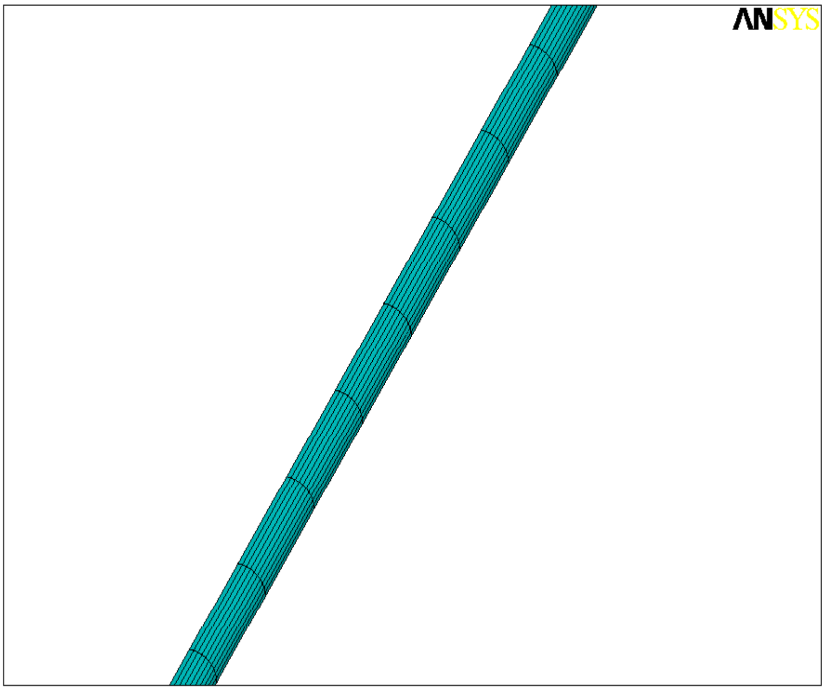

Figure 4: Example mesh for a given superconductor geometry. (Notice regular line intervals)

Everything else in the pre-solving process is standard for any ANSYS simulation: volumes are created and then modified in the current version of the program through volume overlap operations, material properties are applied to the volumes as the user sees fit, and the mesh is created through a mesh sweeping command. The important pieces of information in the pre-solving method that need to be extracted and used in the solving method are the material property numbers and the node spacing on the z-axis. This is because the solving method needs to make the distinction between the matrix material and the superconducting material, and with only these two pieces of information can it simulate current sharing behavior in the magnet using a series of macros which are presented in detail in the solving section.

Also of note is the fact that, for cases of symmetrical quench, the user can in fact cut down the geometry of the simulation to 1/8th of the actual case. The reason this can be done is due to zero heat flux between thermally symmetrical boundaries in a thermodynamic system. Since the temperature on the boundaries of the symmetrical surfaces would be the same at all timesteps, no transference of heat would occur (due to the zeroth law of thermodynamics), and the situation would be equivalent to the heat being isolated in the section, as the tested cases reflect.

Solving method

The method of simulation solving is based on mathematical principles: it employs “differentials” that perform the solution in tiny steps to preserve numerical stability and provide correct descriptions of the behavior of the superconductor. The actual value of these differentials is parametric: this allows the user to select the most efficient value in terms of accuracy and time-efficiency for each individual case of quench, and to alter it for any subsequent cases to be tested. These “differentials” are both spatial and temporal, and a programming flowchart describing how these contribute to the solution process is presented below.

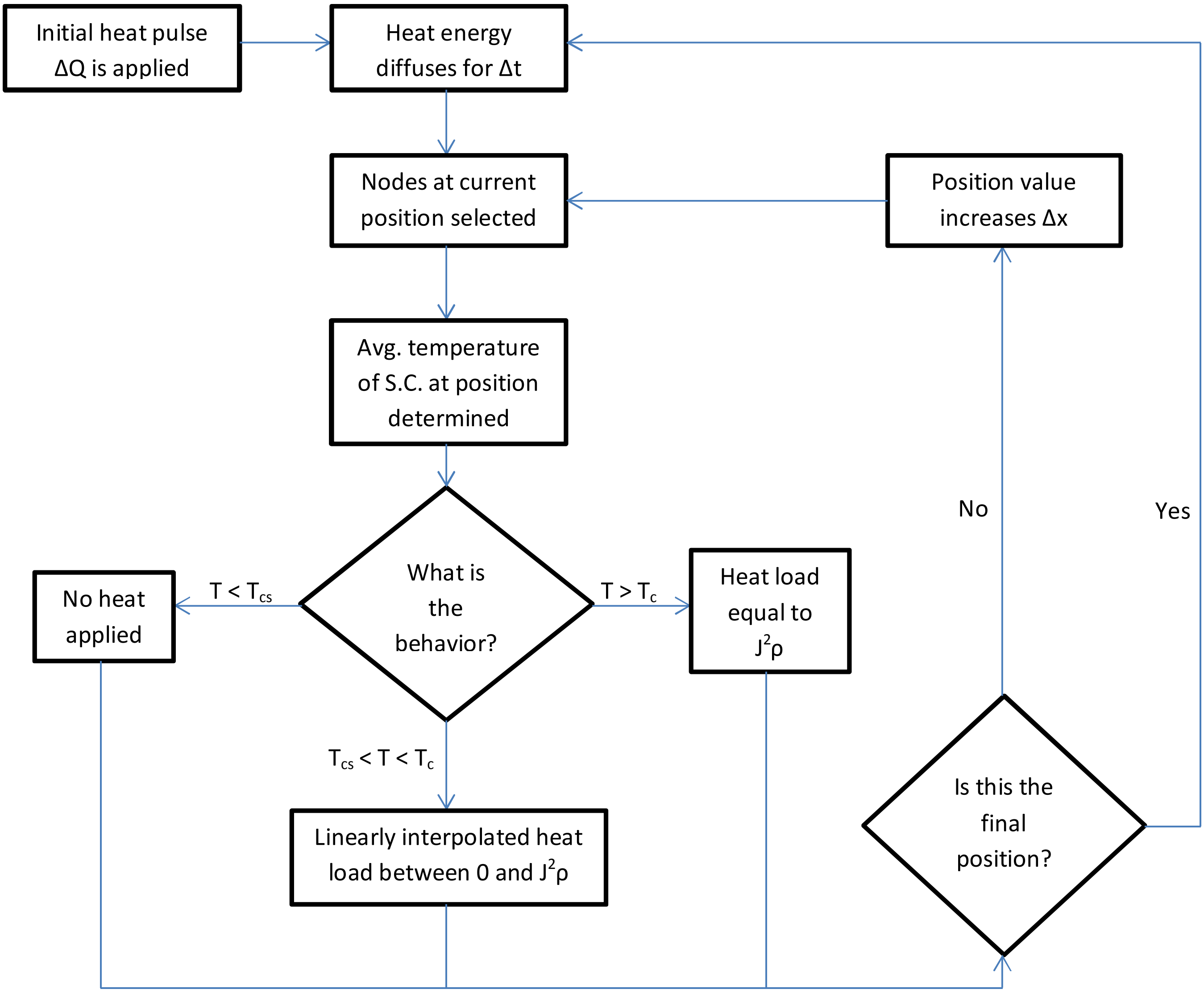
Initial heat pulse ΔQ is applied
Heat energy diffuses for Δt
Nodes at current position selected
Position value increases Δx
Avg. temperature of S.C. at position determined
What is the behavior?
T < T_cs
No heat applied
T > T_c
Heat load equal to J²ρ
T_cs < T < T_c
Linearly interpolated heat load between 0 and J²ρ
Is this the final position?
No
Yes

Also incorporated into the program is a piece of code that adjusts the timestep if the solution does not converge properly: if the program detects the solution will not converge, it will divide the timestep in half and attempt to solve it until it finds a timestep that converges. It will then continue solving with this new timestep, but if the solution for the next timestep converges quickly enough, it will increase the size of the timestep slowly until it goes back to the normal timestep assigned by the user.

Tested cases

Single-strand case

The single-strand case represents a composite strand with a single superconducting niobium-titanium core and a copper stabilizer matrix, where the ratio of copper stabilizer to niobium-titanium superconductor is 1.3 to 1. In an actual sample, the superconducting core is not a single entity; it is composed of small filaments that together make up a filament bundle in the rough shape of the core modeled. The core model was chosen to significantly increase time-efficiency without compromising result accuracy: any interaction between the matrix and individual filaments as compared to the core model would have been extremely negligible.

This single-strand model also represents a situation where the magnet is not surrounded by coolant, and all heat energy resides entirely in the magnet. Symmetry was exploited in the development of the model; since the quench is symmetric as well, only one-eighth of the geometry had to be actually created. However, this has to be taken into account when calculating MQE, since the applied ΔQ is one-eighth of the actual value that is being simulated. In the current version of the program, this is automatically calculated: however, for customization of the program in which quenches are asymmetrical, this should be noted.

This single-strand analysis is very useful for testing materials themselves: outside interference from insulators may compromise result validity, and the near-adiabatic condition of the hot spot allows for good comparisons with the temperature values predicted by the MIITS method. Therefore, testing the accuracy of the simulation itself should be done with the single-strand analysis. Luckily, efficiency of solving-time for the single-strand case has been very fruitful: it takes less than 2 minutes to successfully verify a MQE value to a margin of maximum 5 μJ of error (assuming the user makes a reasonable initial guess.)

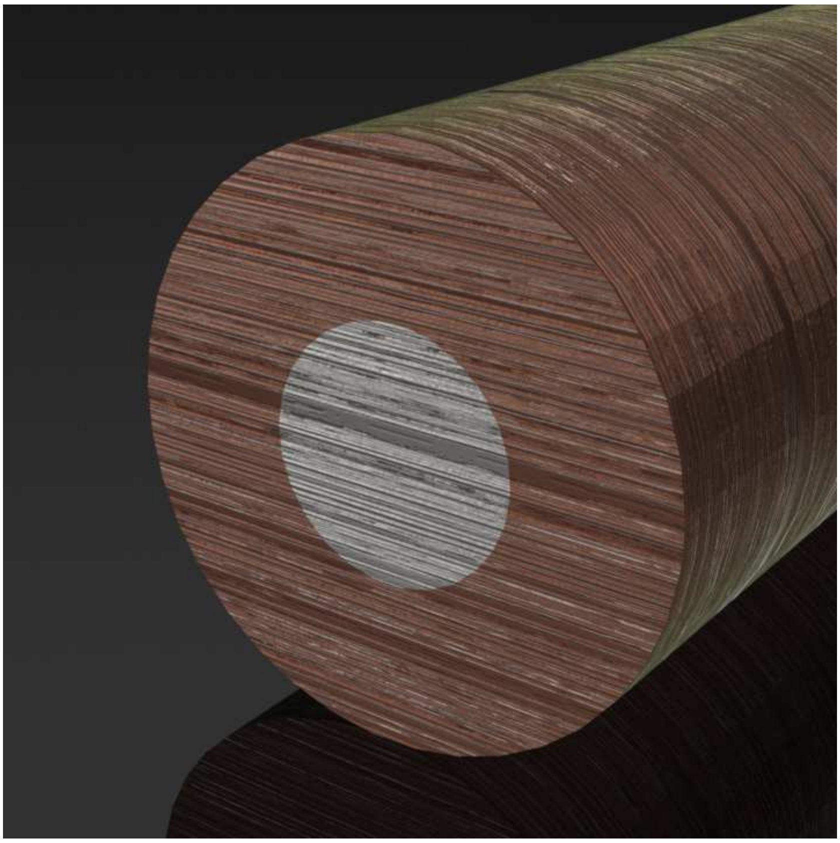

Figure 5: Geometry of Cu/NbTi superconductor used

Multi-strand case

The multi-strand case represents a cable pack, where multiple identical composite strands are evenly spaced inside of a G-10 thermal insulator. This permits the observation of the effect of a thermal insulator around a quenching material, and, if time had permitted, different thermal behaviors by altering the localization of quench in the cable pack. The simulated cable pack is 3x3, with symmetry conditions exploited to build only one-eighth of the geometry (like in the single-strand case). Accordingly, only one-eighth of the declared initial quench energy is actually applied, also like in the single strand case.

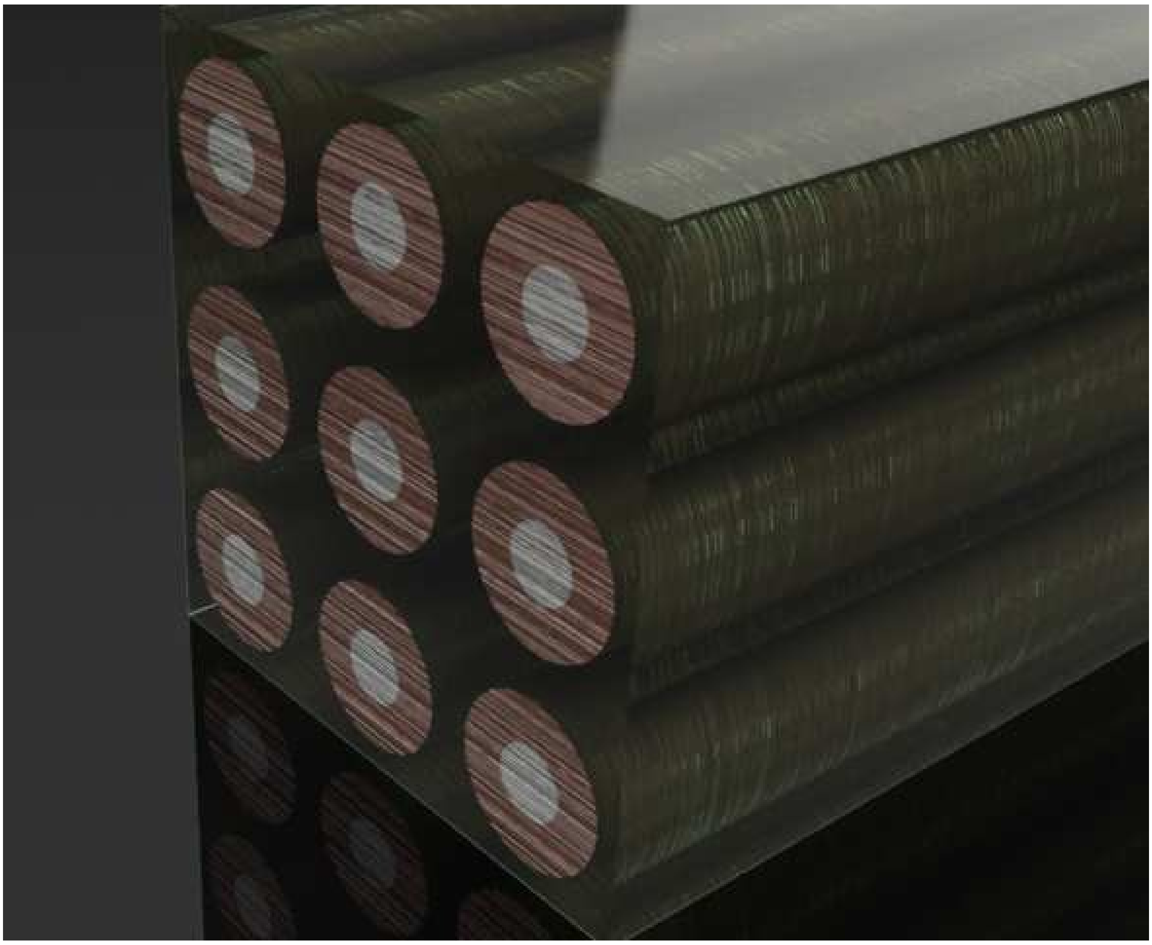

Figure 6: Geometry of Cu/NbTi strands in G-10 epoxy used

The multi-strand simulation may be considered a “hard” alteration to the program, in contrast with “soft” alterations like changing the operating current, changing the disturbance spectrum, or tweaking the size of previously existing geometry: by adding more strands, the program then has to take into account the presence of each individual strand and establish a distinction between them. If this did not happen, the program would consider the individual strands like one coupled entity and perform delocalized calculations, leading to unphysical behavior. However, the solving method does not need to be altered; by assigning different material numbers to the strands (but retaining the same material properties), each individual strand is analyzed one-by-one and correct behavior is displayed in the simulation.

Since the geometry in this case is considerably more complicated than in the single-strand case, the solution time is of course longer. However, the memory requirement for the solving process to run entirely in-core is approximately 500 MB (depending on the initial quench energy), allowing for a computer with even 2 GB of RAM to solve the simulation at the fastest possible speed. The quench in this case was applied to the center strand; this allows for quench symmetry and cuts down the amount of geometry used severely, rendering the time-efficiency mentioned before.

Results

FEA vs. MIITS

The following is an exemplary comparison of the thermal behavior in a quench event, as predicted by the MIITS method and as observed in the simulation. The demonstrated graph represents the MIITS prediction and the FEA simulation values for the maximum hot spot temperature in the previously described single strand case where the operating current is at 75% of critical current. The time interval shown in the graph represents the start of the quench event until the normal zone propagates across the entire conductor, making it normally resistive. After this point it can be assumed that due to the externally adiabatic condition of the simulation, the magnet has invariably quenched since the heat energy cannot spread anywhere else. Accordingly, no stability parameters can be calculated from the analysis after the given time interval for this particular case, and no time need be wasted on calculating the behavior of the system afterwards. (It is interesting to note the quickness of the process: at 75% operating current percent, the magnet fully quenches in little more than 10 milliseconds.)

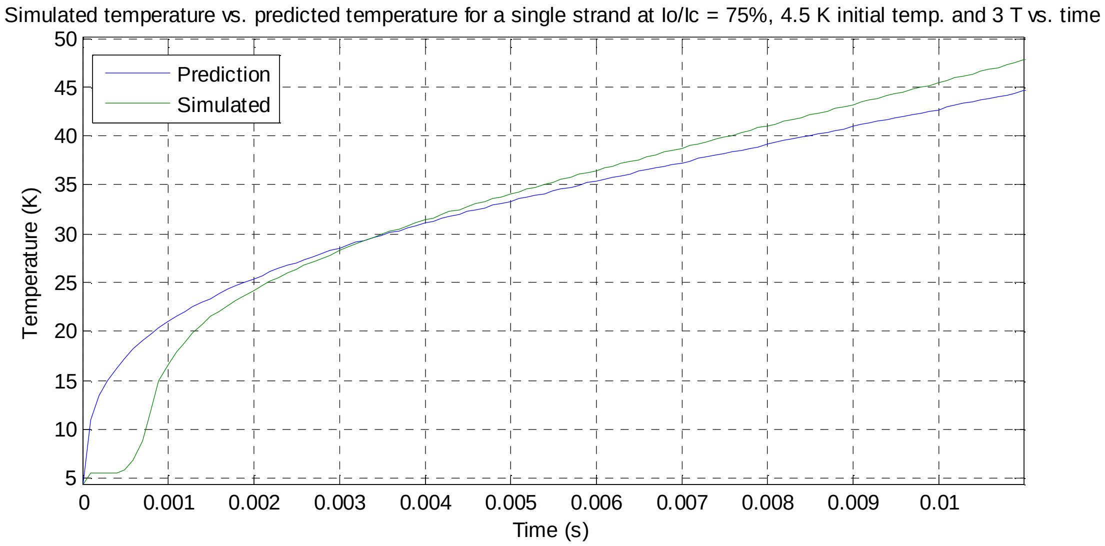

Figure 7: Predicted (MIITS) vs. simulated (ANSYS) hot spot temperature as a function of time

The graphs indicate two differences of note: the initial drastic deviation of behavior in the simulated case during the initial stages of the quench, and the slightly larger value of the simulated temperature versus the predicted in the latter parts of the quench. The former is due to current sharing behavior: since the quench is initiated with energy barely above the MQE, the initial heat pulse is not enough to create large enough Joule heating to raise the maximum temperature of the hot spot and the temperature decreases due to thermal conduction. However, this heat is conducted not only longitudinally, but also transversally into the superconductor, causing more current to flow out of the superconducting core and into the matrix. This generates, in turn, more Joule heating, and this cycle continues until normal quenching behavior occurs (as seen in the graph.)

The latter behavior is a lot more difficult to pinpoint precisely; since the predicted temperature of the strand excludes thermal conduction, one would expect the simulated temperature to always be lower than the predicted. The sensible reason why this behavior is occurring is due to the fact that the magnet is not homogeneous: the separate entities of the superconductor and the matrix create a thermal “lag” in which the heat energy being generated by the matrix does not immediately diffuse equitatively into the superconductor. This can cause the temperature of certain sections of the matrix to be a bit higher than the superconductor, and this possibly leads to the behavior shown. Whether or not this is entirely responsible for the shape of the curve requires experimental verification.

Minimum Quench Energy

Various simulations were run to determine the minimum quench energy in the single strand at various operating conditions: below are the results, accompanied by a datafit.

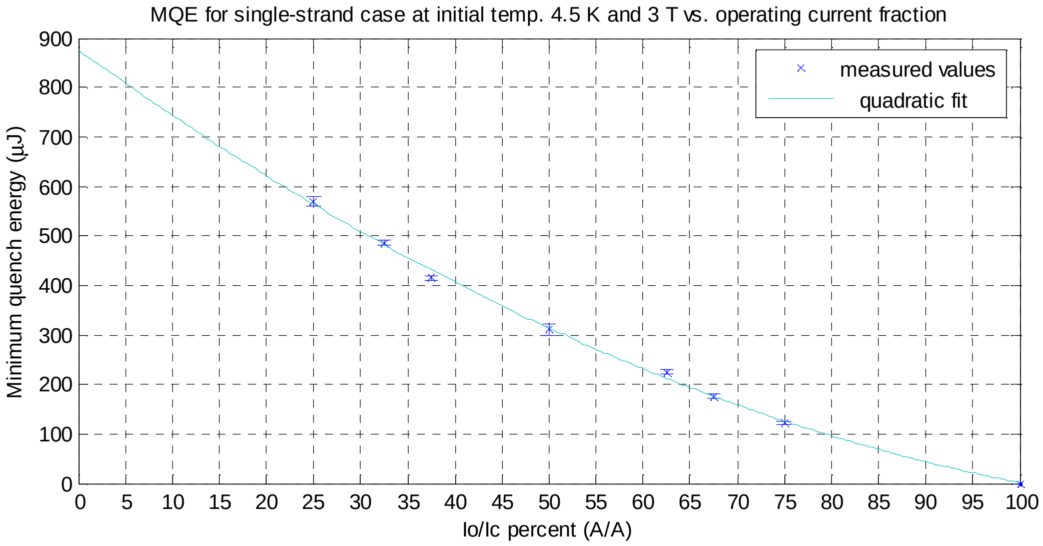

Figure 8: MQE values for single-strand as a function of operating current percent

The values indicate a slight nonlinearity in the values of the minimum quench energy as a function of the operating current, but the MQE does monotonally decrease as the operating current increases (as expected). It is of note to mention that the data fits in very well with a quadratic curve: whether or not the entire operating current region fits into this curve, however, is yet to be determined.

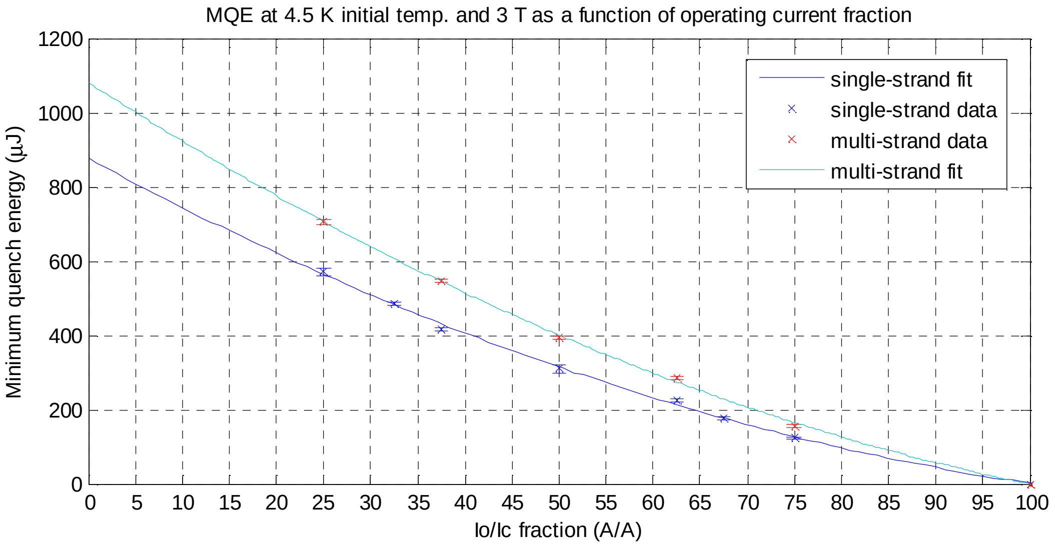

Figure 9: MQE results for single and multi-strand simulations

Both the single-strand and the multi-strand case data fit quadratic curves, as can be clearly observed. Whether or not this holds for all regions (as in the single-strand case), or whether or not the regions where it wouldn't hold are different in the two cases, is yet to be seen. However, we can deduce a general behavior due to the data points already calculated. The multi-strand case at measured values indicates a uniform 25% increase in MQE compared to the single-strand case. This indicates that the insulator always increases the MQE value by a uniform 25% percent.

Conclusions

From the results we can see that the simulation is self-consistent: that is, the results one case produces compared to another seem physically correct. The insulator increases the MQE of the strand by a uniform 25%, an expected result, and the MQE monotonically decreases as operating current increases for both tested cases. The simulation and the MIITS prediction also seem to agree where they need to, emphasizing a need to represent current sharing behavior correctly to be able to determine these cryostability parameters efficiently. However, whether or not these values agree with the experimental real-world equivalent is yet to be seen, and should be the next step forward in the development of the program.

Future use

Now that the program is proven to be self-consistent, all we need is experimental verification of the results to confirm the validity of the data produced. After this, the uses are nearly limitless: we can simulate quench in high-temperature superconductors, for example, to aid the development of new magnet-grade materials which can be used for future higher-field experiments (like the Muon Collider). We can also optimize the amount of insulator used in an experimental configuration to avoid overengineering by testing various cases in the simulation, saving critical funds and time. This can apply to any aspect of the design, from the operating current to the ratio of matrix to superconductor. Hopefully, this program's use can extend even beyond accelerator magnet design and be tested for high-field medical machinery like MRI's, not a big step at all.

Acknowledgements

I'd like to thank my supervisor, Tengming Shen, for his patience with me while I learned the ups and downs of finite element analysis, and for trusting me with such an ambitious project. He's served as an excellent guide through the world of accelerator technology, and I could not have completed this project without him.

I'd also like to thank my mentors, Dave Peterson and Elmie Peoples-Evans, and the SIST Committee for not only providing me with the opportunity to perform science at the frontier of human knowledge, but for helping me and accommodating me so well while I was doing it. My time at Fermilab was wonderful

both in the laboratory and out, and it wouldn't have been possible without their coordination and dedication to the program.

At the root of this, I have to thank the laboratory itself. It's not very often that you find an institution that dedicates itself to science education just as much as it does to science, and providing undergraduate students with the opportunity to contribute to the major physics discoveries of the era is amazing in and of itself. The consistent dedication the laboratory shows to providing young people with scientific knowledge and research opportunities even during times of austerity place it at an exemplary position in the national laboratory system and ensures its livelihood for decades to come.

References

Asner, F. M., 1999, *High-Field Superconducting Magnets,* Oxford University Press, New York, 264 p.

Dresner, L., 1995, *Stability of Superconductors,* Plenum Press, New York, 225 p.

Iwasa, Y., 1994, *Case Studies in Superconducting Magnets,* Plenum Press, New York, 512 p.

Wilson, M.N., 1987, *Superconducting Magnets,* Oxford University Press, New York, 352 p.